NBSIR 81-2403

Gallium Arsenide Materials Characterization: Annual Report, October 12, 1978 to October 12, 1979

U.S. DEPARTMENT OF COMMERCE
National Bureau of Standards
National Engineering Laboratory
Center for Electronics and Electrical Engineering
Semiconductor Materials and Processes Division
Washington, DC 20234

December 1981

or

. Army Electronics Technology and Devices Laboratory
nmouth, NJ 07703

NBSIR 81-2403

GALLIUM ARSENIDE MATERIALS CHARACTERIZATION: ANNUAL REPORT, OCTOBER 12, 1978 TO OCTOBER 12, 1979

J. R. Ehrstein and A. C. Seabaugh

U.S. DEPARTMENT OF COMMERCE
National Bureau of Standards
National Engineering Laboratory
Center for Electronics and Electrical Engineering
Semiconductor Materials and Processes Division
Washington, DC 20234

December 1981

Prepared for
The U.S. Army Electronics Technology and Devices Laboratory
Fort Monmouth, NJ 07703

U.S. DEPARTMENT OF COMMERCE, Malcolm Baldrige, *Secretary*
NATIONAL BUREAU OF STANDARDS, Ernest Ambler, *Director*

CONTENTS

LIST OF FIGURES

LIST OF FIGURES (continued)

LIST OF TABLES

Gallium Arsenide Materials Characterization

by

J. R. Ehrstein and A. C. Seabaugh

Semiconductor Materials and Processes Division
National Bureau of Standards
Washington, DC 20234

ABSTRACT

Ohmic and Schottky barrier contacts for use in electrical characterization were examined both conceptually and experimentally with particular focus on the problems associated with ohmic contacts to semi-insulating GaAs. The conductivity type of the semi-insulating material, which can be either n- or p-type, was investigated by means of a potential profiling technique. In addition, the feasibility of spreading resistance measurements was examined and applied to both low resistivity bulk GaAs and ion-implanted semi-insulating substrate material.

Key words: contacts; gallium arsenide; potential profiling; spreading resistance.

1. INTRODUCTION

The superior electronic properties of gallium arsenide (GaAs) for the fabrication of high-speed digital, microwave, and optoelectronic devices and circuits are required in a number of government and industrial applications. However, there are many unsolved problems in materials growth, material characterization, device fabrication, and device characterization which must be surmounted before the full potential of GaAs can be realized. This report is concerned with the material characterization aspects of these problems, in particular the nature of metal semiconductor contacts for transport measurements and spreading resistance measurements.

2. ELECTRICAL CONTACTS TO GALLIUM ARSENIDE

2.1 Introduction

A nontrivial part of any electrical characterization program is the development of reliable and reproducible contacting techniques. Care must be taken to ensure that the formation of contacts does not alter the properties of the material or adversely influence the desired characterization technique. It is well known that arsenic dissociates from a GaAs surface during heat treatments at temperatures as low as 300°C. Since the effective sintering temperature of most contact metals is greater than 300°C, there are unique problems in contacting GaAs. Processing temperatures must be kept as low as possible, and the specimen must be kept at these temperatures for as short a time as possible in order to minimize this problem.

In general, metals and alloys for making ohmic* contacts to semiconductors are chosen on the basis of two guidelines [1]: (1) a material of high work function is chosen for *p*-type material and low work function for *n*-type material and (2) the metal should form a region of high majority carrier density under the contact after an appropriate alloy cycle. If these guidelines are followed, the width and height of the metal-semiconductor potential barrier is reduced, thus increasing the probability of conduction by both thermionic emission over the barrier and tunneling through the barrier. Conversely, metals for Schottky barriers† are chosen for (1) their low work function for *p*-type material and high work function for *n*-type material and (2) their inability to form a high carrier density region under the contact. These guidelines lead to large barrier width and height, thereby decreasing the probability of thermionic emission over the barrier or tunneling through the barrier. For GaAs, the barrier height is only weakly dependent on the metal work function due to the high surface state density which pins the Fermi level at the metal-semiconductor interface. Therefore, the properties of Schottky-barrier contacts to GaAs are only a weak function of the metal used.

Semiconductors can be divided into three categories which distinguish between the dominant effects determining the Fermi level position at the contact interface [2].

1. The Fermi level at the interface is a function of metal work function, semiconductor electron affinity, and semiconductor doping (e.g., cadmium sulfide).

2. The Fermi level is pinned at the surface due to intrinsic surface states (e.g., germanium, silicon).

---

* In this work, an ohmic contact is defined as a metal-semiconductor contact exhibiting negligible voltage drop with respect to the device voltage. For example, in the case of two similar contacts formed on a bulk semiconductor, a linear current-voltage characteristic, with current passing through the contacts and the voltage measured across the contacts (over a voltage range typical for the device), is termed ohmic.

† In this work, a Schottky barrier contact is defined as a metal-semiconductor contact (i.e., not a *p*-*n* junction contact) whose current-voltage characteristic can be approximated by the relation

$$I = I_s \left(e^{\frac{qV}{kT}} - 1 \right),$$

where I is the current in A, I_s is the reverse bias saturation current in A, q is the electron charge equal to 1.602×10^{-19} C, V is the voltage applied across the contact in V, k is the Boltzmann constant equal to 1.38×10^{-23} J/K, and T is the absolute temperature in K. A Schottky barrier contact can often be distinguished from a *p*-*n* junction contact by the absence of minority carrier injection under forward bias conditions.

3. The Fermi level is pinned at the surface due to extrinsic surface states (e.g., gallium arsenide, indium phosphide, aluminum antimonide).

For a category 1 semiconductor, the barrier height, $q\phi_B$, for electrons and holes, respectively, is described by [3],

$$q\phi_{B_n} = q\,(\phi_m - \chi) \qquad \text{for } n\text{-type semiconductors}$$

$$q\phi_{B_p} = E_g - q\,(\phi_m - \chi) \qquad \text{for } p\text{-type semiconductors}$$

where $q\phi_m$ is the metal work function in eV, $q\chi$ is the semiconductor electron affinity in eV, and E_g is the energy band gap in eV. Schottky barrier image force lowering has been neglected in these expressions, but could easily be included without qualitatively altering the discussion. In principle, a metal work function can be chosen such that $q\phi_{B_n} = q\phi_{B_p}$, thus

$$q\phi_m = \frac{E_g}{2} + q\chi \ .$$

For this choice of metal work function, a barrier contact will be formed to the semiconductor independent of the conductivity type. This is desirable in potential profiling measurements to determine the conductivity type of category 1 semiconductors.

When the Fermi level is pinned at the metal-semiconductor interface by surface states as in categories 2 and 3, the Schottky barrier height is given by the difference between the majority carrier band edge and the energy level at which the Fermi level is pinned, E_{FP}, in eV. For n-type material, this is

$$q\phi_{B_n} = E_c - E_{FP} \ ,$$

where E_c is the conduction band edge in eV. For p-type material

$$q\phi_{B_p} = E_{FP} - E_v \ ,$$

where E_v is the valence band edge.

Using this simple model, then, and the fact that the Fermi level at the GaAs surface has been found to be pinned at roughly midgap [4,5,6], a metal-semiconductor contact to n- or p-type GaAs will typically form a Schottky barrier contact. To form an ohmic contact, a region of high majority carrier density must be formed under the contact. This highly doped region increases the probability of carrier transport by tunneling through the barrier. If this results in a negligible barrier voltage drop with respect to the device voltage drop, the contact is termed ohmic.

2.2 Contacting and Profiling Experiments

There are a wide variety of techniques available for forming ohmic contacts to GaAs. Among the most simple techniques are alloy regrowth and ultrasonic soldering. In this work ohmic contacts were formed by both of these techniques.

For the alloy regrowth method on n-type specimens ($N_d - N_a \geq 10^{16}$ cm^{-3}), alloying was performed on a tantalum microstrip heater purged in an electronic grade forming gas atmosphere (95 parts nitrogen, 5 parts hydrogen by volume). Typically, the GaAs specimen was prepared by rinsing successively in trichlorethylene, acetone, and methanol followed by a 1-min etch in a room temperature sulfuric acid-peroxide solution (3 parts sulfuric acid, 1 part hydrogen peroxide, 1 part deionized water by volume). The specimen was then rinsed in deionized water and blown dry with nitrogen prior to placement on a high purity graphite boat which provided physical isolation from the tantalum heating element. Indium, tin, or indium-tin alloy spheres of 20-mil (0.51-mm) diameter were etched in hydrochloric acid and placed directly onto the GaAs surface through holes in a graphite mask used to align the spheres and to prevent their rolling off. The system was subsequently purged for 10 min at a flow rate of roughly one liter per minute before alloying. Temperature was monitored by means of a type K thermocouple which was spot welded to the bottom of the tantalum strip, and the process was continuously observed through a microscope. In a typical process sequence the temperature was increased until the spheres melted and collapsed, the specimen was alloyed for 30 s at the collapse temperature, the power in the tantalum heating element was then turned off, and the system was allowed to cool to room temperature. The contacts formed by this technique were found to be ohmic and suitable for electrical transport measurements.

Alloy regrowth ohmic contacts were also formed to n-type specimens after an electroplating technique described by Mattauch [7]. In this ohmic contact process, a three-layer structure is utilized: tin-nickel, nickel, and gold. The tin-nickel alloy is pulse-electroplated at approximately 1 A and 1 Hz (with a 50-percent duty cycle). This layer is followed by a 1-min 20-mA dc nickel electroplate and finally a 1-min 20-mA dc gold electroplate. The tin-nickel/nickel/gold structure is then microalloyed in forming gas at approximately 200°C for 30 s. The contacts fabricated by this process were also ohmic and used for single-probe response studies in the spreading resistance experiments of section 3.5.

Ohmic contacts are often desired on semi-insulating GaAs. In practice, this is more difficult to achieve than for lower resistivity material. It is desirable to know the conductivity type of the GaAs in order to make a suitable choice of contact metal (i.e., so as not to form a p-n junction). Conventional thermal-probe conductivity type determination on semi-insulating material is often ambiguous due to the very low carrier density and resultant small Seebeck voltage. Wolfstirn and Focht [8] have reported on a thermoelectric n-p tester for use on GaAs and gallium phosphide (GaP) using an ac bias to set up an imbalance between back-to-back hot and cold Schottky barriers.

A method recently described by Neumark *et al.* [9] for conductivity-type determination with application to high-resistivity material is potential profiling. According to this method, the conductivity type of a semiconductor can be determined by the potential profile between two barrier contacts across which a voltage is applied. By potential profiling, the preferred direction of electron transfer across the barrier is known with respect to the applied bias. This preferred electron transfer direction depends on the majority-carrier conductivity type, assuming that the dominant transport

mechanism is by thermionic emission over the barrier. It is asserted that by knowing the direction of preferred electron transfer and the polarity of the applied bias, the conductivity type can be determined. This method is illustrated in figure 1 for both *n*- and *p*-type semiconductors. An energy band diagram for the case of two symmetric barrier contacts to *n*- and *p*-type semiconductors under thermal equilibrium conditions is shown in figure 1a. The energy band diagrams change as depicted in figure 1b when the same voltage is applied across these barrier contacts with the polarity shown. Note that for the same polarity of applied voltage, V_A, the left-side barrier contact on the *n*-type material is forward biased, while the left-side barrier contact on the *p*-type material is reverse biased. Similarly, the right-side barrier contact on the *n*-type material is reverse biased, while the right-side barrier contact on the *p*-type material is forward biased. By profiling the potential between the two-barrier contacts, these conditions can be detected and the conductivity type determined. Figure 1c displays the expected potential profile (with voltage measured with respect to the left-side barrier contact) for both the *n*- and *p*-type cases. The voltage drop due to the specimen bulk resistance is represented by V_R.

Potential profiling can be implemented by using an array of barrier contacts formed on the high resistivity material. A schematic diagram of this measurement is shown in figure 2. A voltage, V_1, is applied to the Schottky barriers at opposite ends of the specimen (contacts labeled 1 and n) and the resulting voltage distribution is measured as the voltage, V, at the intermediate contacts, after adjusting V_2 for zero current through the ammeter, A. In this manner, no current is drawn from the specimen in the voltage measurement circuit, and an accurate determination of the potential of each of the contacts can be made.

The apparatus (as shown in fig. 2) was assembled and the technique verified on a 2 Ω•cm *n*-type silicon specimen. The measured results are shown in figure 3 which is a plot of contact-to-contact voltage *versus* probed contact position along a line of evaporated aluminum Schottky barrier contacts. As depicted in figure 2, three probes were used to contact the specimen, each consisting of a tungsten wire held in a micropositioner. Two probes used to bias the specimen were placed on the end contacts and remained fixed, while the third and central probe was used to probe the potential from left to right. For the initial profile, with polarity as indicated in figure 2, the potential was measured between the left-side end contact (i.e., contact #1 in fig. 2.) and the central probed contact. The current was then reversed and the potential reprofiled with voltage measured with respect to the right-side end contact. In figure 3, the initial profile of the specimen corresponds to that expected for *n*-type material and shown previously in figure 1c. When the current is reversed, the end contacts reverse roles: the leftmost contact becomes reverse biased, while the rightmost contact becomes forward biased as indicated in the potential profile of figure 3. By comparing the initial profile of figure 3 with the potential profiles expected (fig. 1c), it is verified that the silicon specimen is *n*-type.

Results of applying this technique with evaporated gold Schottky barrier contacts on semi-insulating GaAs are shown in figure 4. For the initial profile with polarity as indicated in figure 2 and central probe stepped from left to right, the potential difference between contacts 1 and 2 is greater

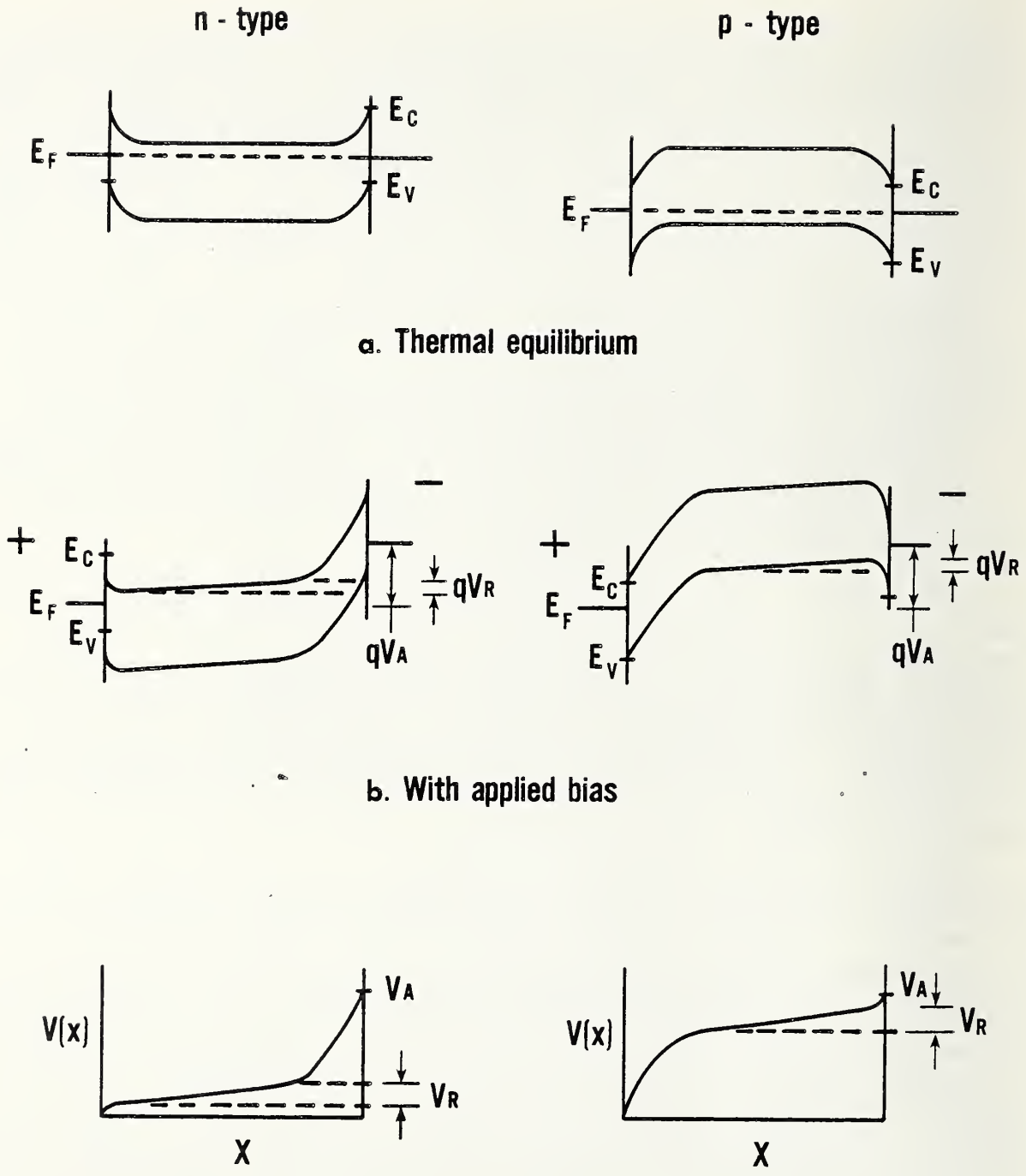

Figure 1. Schematic summary of the potential profiling technique. (a) Energy band diagram plotted against position for two metal-semiconductor barrier contacts on *n*- and *p*-type semiconductors in thermal equilibrium. (b) The same systems with applied bias (V_A) as specified. V_R is defined as the voltage drop in the bulk region of the semiconductor. (c) Potential profile, V, also plotted against position.

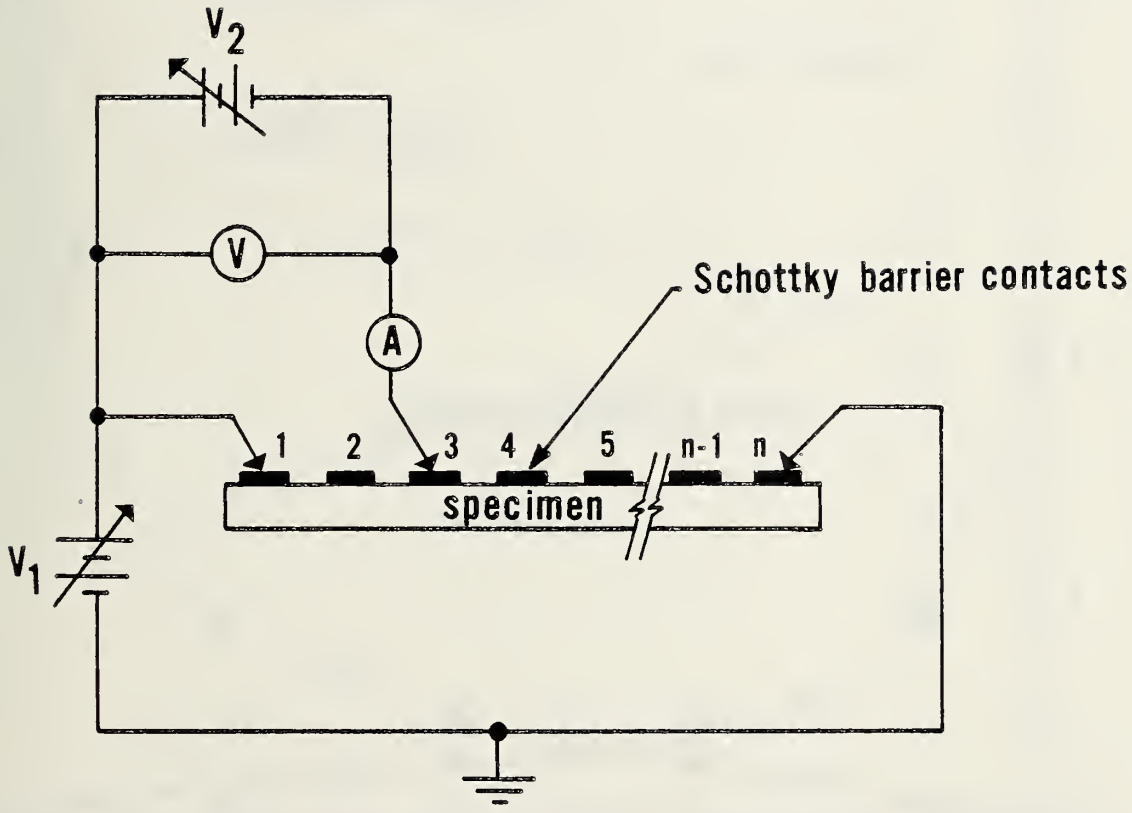

Figure 2. Schematic diagram of potential profiling circuit.

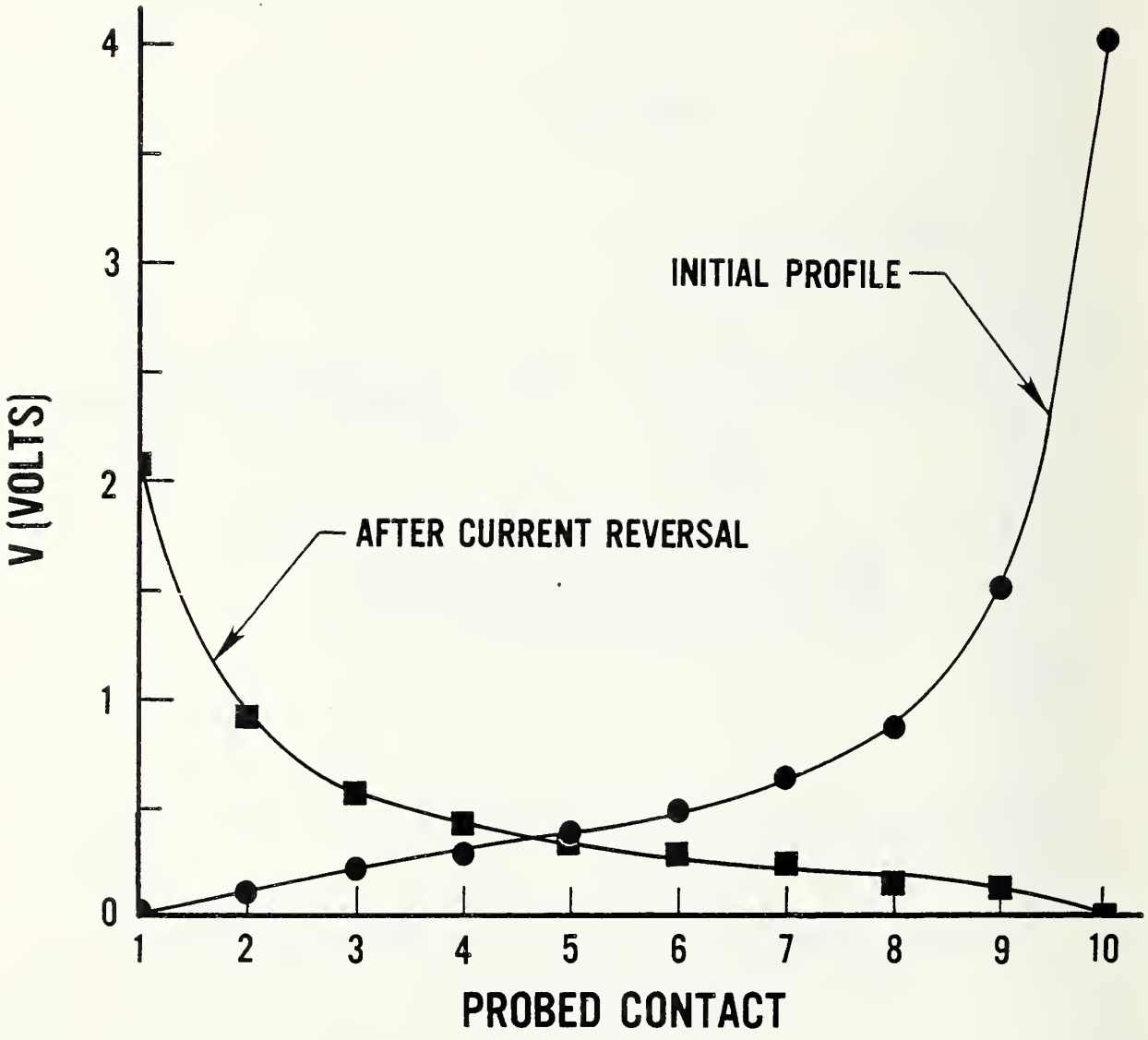

Figure 3. Potential profiles of a 2 Ω•cm n-type silicon specimen. Schottky barrier contact spacing is approximately 15 mil (0.381 mm).

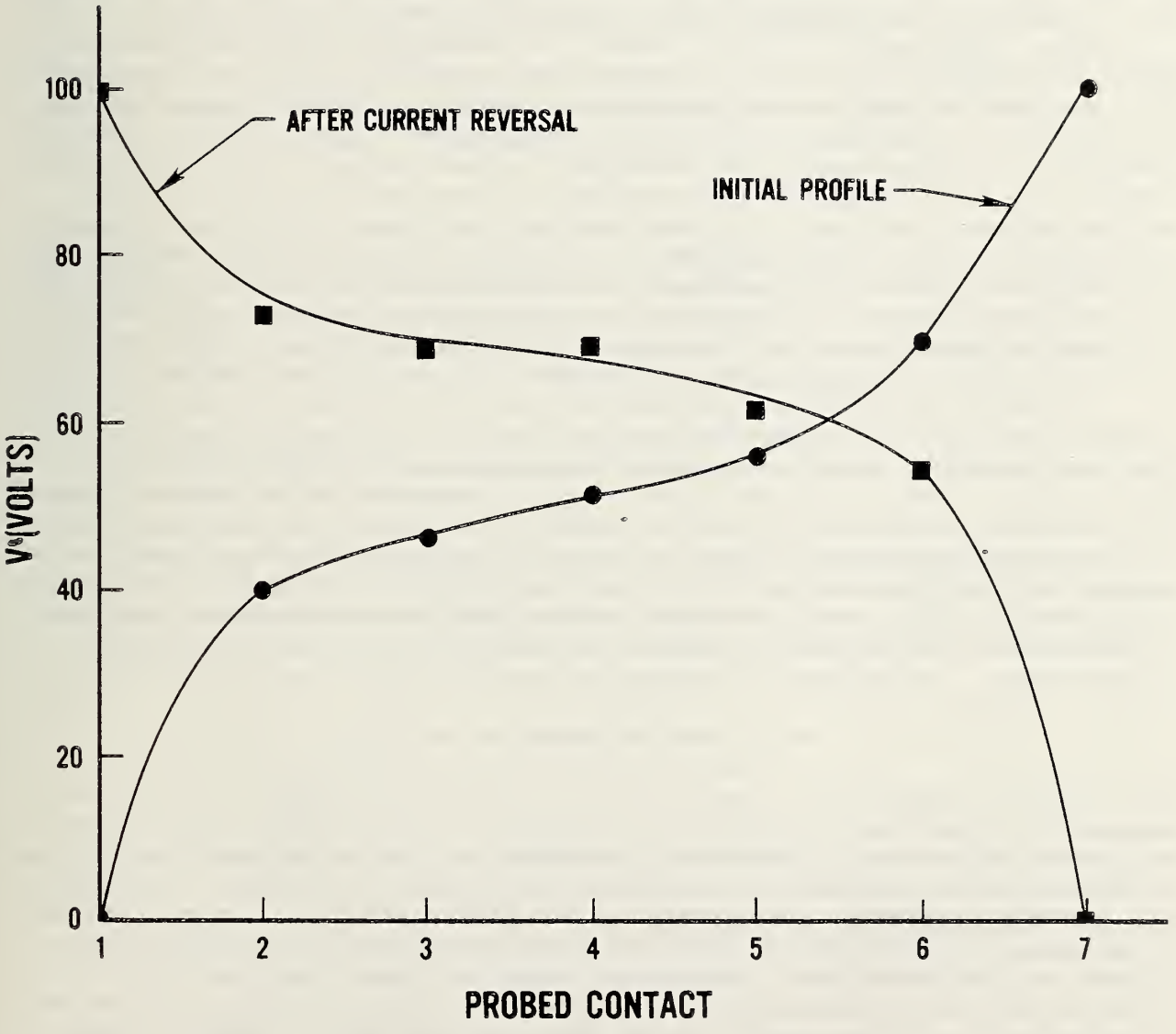

Figure 4. Potential profile of a 10^7 Ω•cm chromium-doped GaAs specimen. Schottky barrier contact spacing is approximately 30 mil (0.762 mm).

than that between contacts 6 and 7 at the other end. When current through the specimen is reversed (and the zero of potential taken at the opposite end, i.e., contact 7), the converse of this situation occurs, with the potential difference between contacts 6 and 7 becoming greater than that between contacts 1 and 2. Note that due to the high specimen resistance the asymmetry is not as pronounced as in the 2 Ω•cm silicon specimen (fig. 3). The result is opposite to that seen in the silicon specimen and for the given polarity of applied bias corresponds to the profile expected for p-type material (see fig. 1c). This p-type conductivity indication was typical of both the undoped and chromium-doped GaAs substrates profiled in this study.

With a knowledge of the semi-insulating GaAs conductivity type, it is possible to select an ohmic contact metal such that a p-n junction is not formed. In this work, alloy ohmic contacts were attempted on semi-insulating GaAs (using the technique previously described) without success, using high purity indium, zinc, and indium:tin (50 parts In:50 parts Sn by weight). Linear current-voltage characteristics were achieved only when the surface converted to low resistivity. Ohmic contacts to semi-insulating GaAs were successfully formed in this work by ultrasonically soldering either indium-tin or indium zinc alloys (50 parts In:50 parts Sn or Zn by weight) at less than 150°C. The specimen was then allowed to alloy on a hot plate in air at 150°C for 5 min. This method, however, was not reproducible for unknown reasons.

Schottky barrier contacts to both low and high resistivity GaAs can be achieved routinely using conventional semiconductor processing techniques. Gold Schottky barrier contacts were formed in this work by dc electroplating and by vacuum evaporation. Electroplated contact definition was facilitated by photolithographically defining an array of holes in a pyrolytically deposited silicon dioxide layer. The gold was plated at 20 mA for 2 min with no subsequent alloy step. Evaporation-deposited Schottky barriers were delineated during deposition by means of a 5-mil (0.13-mm) stainless steel shadow mask.

2.3 Discussion

The problems encountered in making Schottky barrier and ohmic contacts (particularly to semi-insulating GaAs) were examined conceptually and in a few preliminary experiments. Potential profiling as a means of conductivity-type determination was examined and applied to high-resistivity GaAs. In summary, the material properties that affect contact characteristics in GaAs include Fermi level pinning at the surface due to surface states, the surface region doping, and the metal work function (although very weak for GaAs). For the specific problem of forming ohmic contacts, the surface region must be heavily doped to form a tunnelable barrier (e.g., by alloying). However, since this process must be done at low processing temperatures (in order to minimize arsenic out-diffusion), the choice of metals is restricted. This restriction may well be overcome by capping the exposed GaAs surface (e.g., with silicon nitride), laser annealing the metal contact, or some combination of these techniques. Ion implantation may offer the greatest flexibility and control of ohmic contact formation since the surface region over which a contact is to be formed can be heavily doped prior to contact formation. Future study should examine these technologies as well as investigate other ohmic contact alloys such as gold:germanium.

3. SPREADING RESISTANCE MEASUREMENTS

3.1 Introduction

The objective of this subtask is to explore the applicability of the spreading resistance technique to the profiling of ion-implanted layers in GaAs. Although a significant number of papers have been published concerning the methodology and interpretation of spreading resistance measurements in silicon, only three publications address the use of point pressure contact "spreading" resistance measurements in GaAs [12-14]. These papers report measurements on diffused layers and epitaxial structures with multimicrometer layer thickness. However, prior to the present report, no work has been reported on submicrometer thick layers implanted into GaAs.

3.2 Background

The principal difficulty with applying the spreading resistance technique to GaAs is that point pressure contacts using durable alloy probes (tungsten alloys are used to make the measurement on silicon) are neither ohmic nor of reasonably low resistance. In order to use point pressure contacts for resistivity profiling in GaAs, the problem of choosing specimen surface preparation and probe materials to obtain reproducible and acceptable contact properties must be solved. Each of the reported works [12-14] uses a different approach to solving this problem, but none of them was applied to implanted or submicrometer layers.

One of the reported techniques [12] requires special metallization to the probes (which offers reduced contact resistance, but has low durability) and a special contact-forming circuit, while another [13] requires a silver paste metallization stripe for a reference electrode, a large area silver paste backside contact, and a 1-V measurement voltage for profiling. The third technique, reported by Queirolo [14], appears to be the most flexible in that instrumentation and techniques are used which are common for depth profiling of silicon using the spreading resistance mechanism.

Since Queirolo's approach was chosen as the basis for the work reported here, it will be described in detail. Epitaxial and diffused-layer specimens to be profiled were beveled in a thick paste of 0.3-μm alumina in water, using a commercially available polishing fixture intended for preparing specimens for spreading resistance measurements [15]. Following this surface preparation, measurements made with tungsten-osmium probes, each loaded with 45 g, gave acceptably stable measurements with absolute values low enough ($<10^8$ Ω) to be measured with commercial spreading resistance electronics [15]. However, Queirolo reports that the measured resistances are much too large to be characteristic of a spreading resistance; rather the measurement response is dominated by metal-GaAs contact resistance. Ostensibly, the dopant density in the GaAs under the contact controls the barrier resistance, at least in the reported dopant concentration range, 10^{17} to about 5×10^{19} cm^{-3}, and the measured two-probe resistance is approximately inversely proportional to the specimen's dopant density under the contacts. Under these conditions, the geometric spreading resistance is a minor component of the measured resistance, so the sampling volume correction factors normally used to interpret spreading resistance profiles on a graded layer [16,17] are not

needed for measurements of GaAs profiles. As is noted by Queirolo, simple calibration of contact resistance on specimens of known dopant density, which have been prepared in the same manner as the test specimen, is sufficient for profile interpretation.

Although he uses 0.3-μm alumina polishing as a best compromise for both *p*- and *n*-type GaAs layers, Queirolo states that bulk *p*-type GaAs specimens of a given resistivity exhibit better reproducibility and lower contact resistance when measurements are made on surfaces lapped with 5-μm alumina than when made on surfaces polished with 0.3-μm alumina. In contrast to this, he shows that for bulk *n*-type specimens, lower contact resistance and apparently better reproducibility are obtained for measurements made on the polished surfaces. Thus the effect of specimen surface preparation on the resistance measurements, which is perhaps due to specimen damage or to surface state formation, is also apparently a function of specimen conductivity type. (An interactive dependence of measurement quality on specimen preparation and conductivity type - although different in specific details from that shown by Queirolo - was also found in the present work in submicrometer implanted layers and is discussed in secs. 3.5 and 3.6.)

3.3 Limitations Imposed by Commercial Instrumentation

It is desirable to use commercially available spreading resistance equipment for two-probe resistance profiling of GaAs. It is useful, therefore, to consider the normal mode of operation of such a system. The system at NBS is automated and completes a spreading resistance measurement at a position on the semiconductor in a fixed time interval, 6 s in the case of the present measurements. The measurement cycle consists of translating the specimen a preselected increment while the two probes are raised, lowering the probes to the specimen surface with a 10-mV dc bias between the probes at the time of contact, allowing about 1.25 s for the probe contact to settle (or stabilize) to a constant resistance value, electrically sampling the probe-to-specimen contact resistance during a "measurement window," and finally, lifting the probes. The specimen is then translated and the measurement cycle is repeated until the spreading resistance profile of the desired region of the semiconductor is obtained. Figure 5 shows, on an expanded scale, the change of resistance with time and the sequence of probe and stage motions for the case of a pair of probes which do not settle to a constant contact resistance. (This lack of settling of contact resistance is sometimes found with silicon and was very common in the present work on GaAs.) In contrast, figure 6 shows a recorder tracing of the dynamic response, i.e., the log of contact resistance *versus* time, for several measurement cycles with probes having good probe-to-semiconductor resistance-settling characteristics. This tracing was obtained on a 135 Ω•cm *n*-type silicon specimen with a set of tungsten-osmium probes used in the present GaAs study. The ability of the probes to stabilize rapidly is an important requirement for obtaining repeatable data. It is partly controlled by the cleanliness and general condition of the probes, but in the case of GaAs, it was found to be more strongly controlled by the condition of the specimen surface, as will be shown below. A second requirement for obtaining acceptable data, particularly important in the case of GaAs, is that the contact resistance stay below about 10^8 Ω. Although the commercial spreading resistance electronics can obtain accurate measurements of contact resistance up to about 10^9 Ω, the

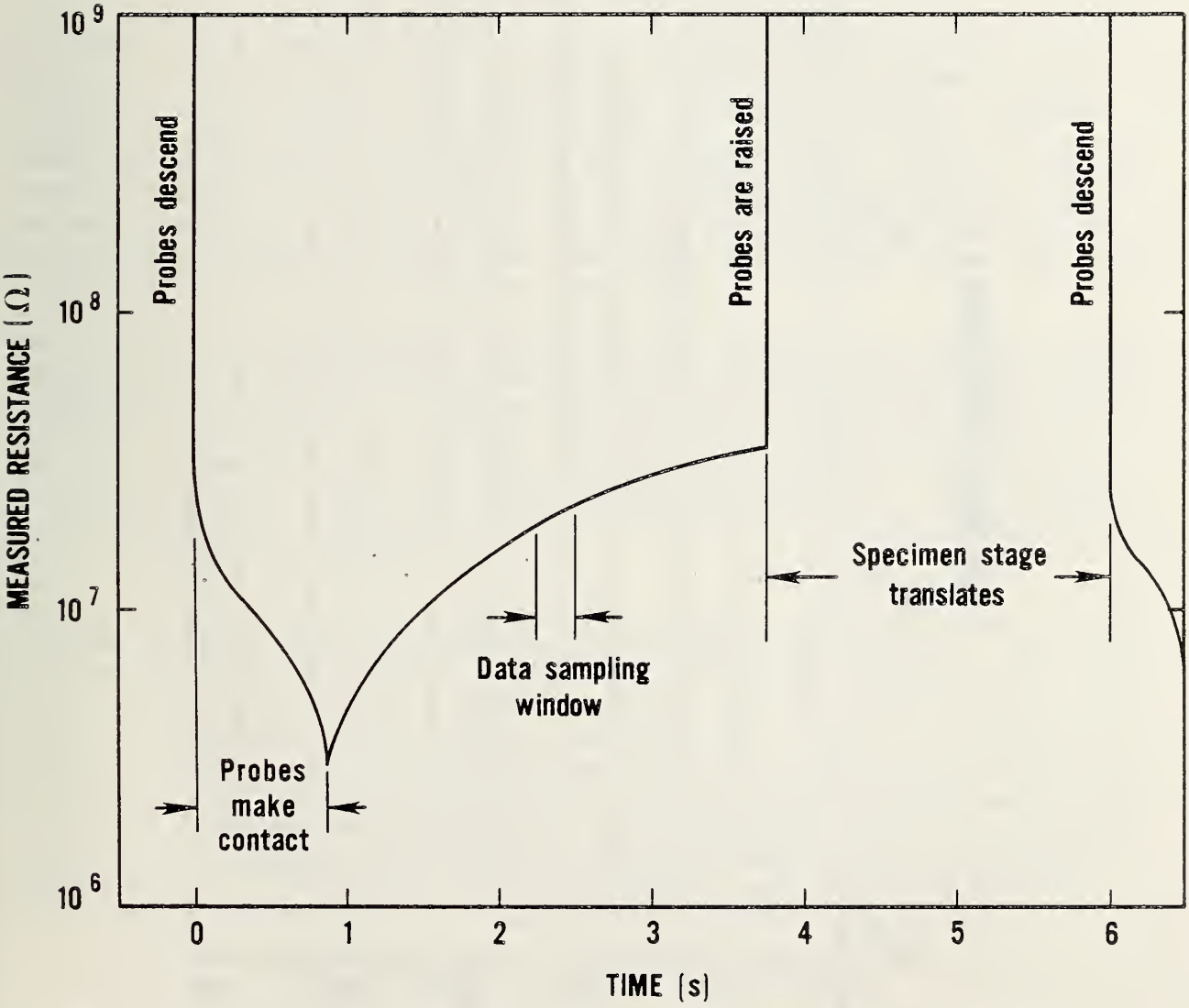

Figure 5. Graph of the measured resistance as a function of time during a single measurement cycle for probes on GaAs showing poor settling characteristics.

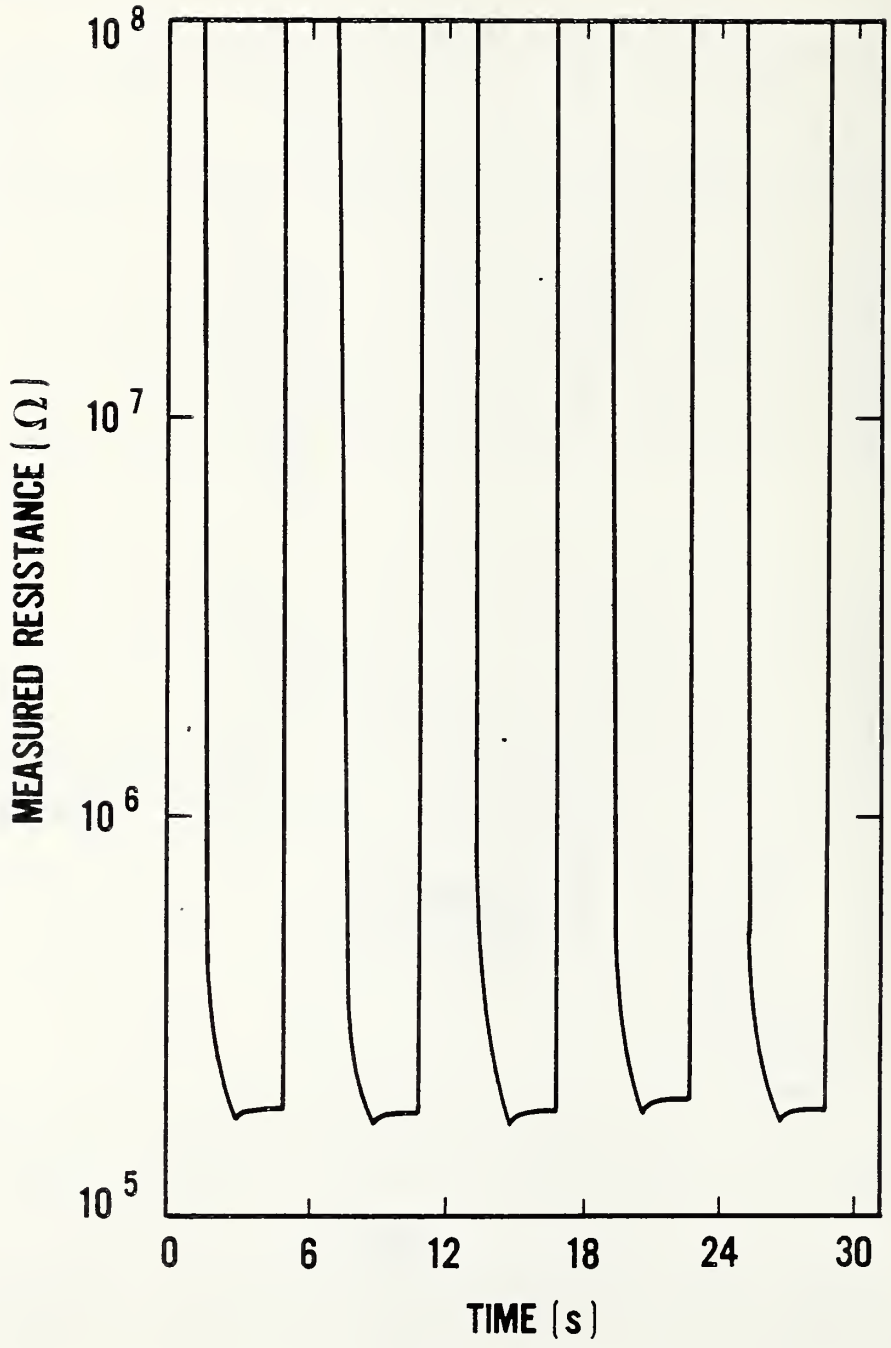

Figure 6. Actual measured resistance for five measurement cycles using a tungsten-osmium probe on 135 Ω•cm *n*-type silicon polished with 0.5-μm diamond. This sample shows good probe-settling characteristics.

time required for the electronics to stabilize increases for resistance values above about 10^8 Ω, and this time may be longer than allowed by the automatic timing cycle. The time requirement for stabilization becomes even more difficult to satisfy if capacitive charging effects are encountered at the probe-semiconductor interface. The practical implication is that resistance readings much above 10^8 Ω on GaAs are suspect since the electronics have probably not stabilized prior to the measurement sampling window (fig. 5).

3.4 Measurement Variables Tested

The experimental factors which control the reproducibility and the general quality of two-probe resistance (spreading resistance) measurements were studied on both bulk and ion-implanted GaAs specimens. Several specimen preparation methods were tested to evaluate their relative effect on contact stability, measurement repeatability, and absolute value of contact resistance. A number of probe materials and a few modifications to the common tungsten-osmium alloy probes were also tested for their effect on the same measurement parameters. Tests were also performed at probe loads from 10 to 45 gf to investigate effects due to probe load.

Tests of specimen preparation methods included alumina polishing and lapping processes, but primary emphasis was placed on the use of various grades of diamond (in the range 0.1- to 6-μm particle size) for specimen polishing and lapping. The reasons for this were twofold: 1) considerable experience in the use of diamond for shallow angle sectioning of silicon specimens exists in this laboratory; and 2) the use of diamond in oil, rather than aluminum oxide in water, was expected to reduce the effect of possible oxide formation on the GaAs specimen surfaces.

Table 1 lists the specimens available for testing. The bulk p-type specimens intended primarily for calibration were received toward the end of the project period and were not fully utilized. Table 2 lists the probes available for the tests. The surface preparation media that were used are listed in table 3. Because of the exploratory nature of this work, not all combinations of specimens, probes, surface preparations, and other operating conditions were tested. The primary emphasis was on identifying the measurement conditions which yielded repeatable results consistent with the measurement limitations of the instrumentation; those probes, probe loads, or surface preparations which appeared to give only erratic results in the initial phases were rejected in favor of more promising ones.

3.5 Experimental Results With Bulk GaAs

a) Effect of Probe Material and Probe Load

The first tests of measurement dependence on experimental conditions were done on bulk (100) silicon-doped (approximately 7×10^{17} cm^{-3}) GaAs using a single tungsten-osmium probe. A large area tin-nickel, nickel, gold ohmic contact (as described in sec. 2.2) was provided on the back surface of the specimen, to complete the circuit. The response of the single probe was checked as a function of load (10, 20, 30, and 40 gf) in both forward and reverse bias on the as-received specimen surface. In forward bias, resistance increased with decreasing load while in reverse-bias no load dependence

Table 1. List of GaAs Specimens Available for Tests.

a. Bulk

Specimen ID	Orientation	Conductivity Type	Dopant	Carrier Density (cm^{-3})
4481	(100)	*p*	zinc	4.5×10^{16}
3284	(100)	*p*	zinc	3.3×10^{18}
4464	(100)	*p*	zinc	4.5×10^{18}
L1723	(100)	*n*	silicon	7.0×10^{18}

b. Ion Implanted

Specimen ID	Substrate Orientation and Type	Conductivity Type of Implanted Layer	Implanted Dopant	Implant Fluence (cm^{-2})	Implant Energy (keV)	30-min (°C)
LDB11	(100) --	*p*	Be	5×10^{13}	100	800
201	(100) n	*p*	Be	5×10^{13}	100	800
203	(100) SI*	*p*	Be	5×10^{13}	100	800
5-434	(110) --	*n*	Se	4×10^{12}	400	800
8163a	(100) --	*n*	Si	5×10^{12}	170	800
8163b	(100) --	*n*	Se	5×10^{14}	300	850

*Semi-Insulating.

Table 2. Probes Available for Test.

Probe Set	Base Material	Modifications, if any
1	tungsten osmium	As purchased with commercial spreading resistance instrument
2	tungsten osmium	Electroplated with rhodium
3	tungsten osmium	Plated with indium-gallium paste
4	tungsten osmium	Ion-implanted with indium at 200 keV to a fluence of 1×10^{15} cm^{-2} and with gallium at 200 keV to a fluence of 1×10^{15} cm^{-2}
5	tungsten osmium	Implanted with gallium at 200 keV to a fluence of 1×10^{16} cm^{-2}
6	tungsten ruthenium	
7	tungsten carbide	

Table 3. Surface Preparation Media Used.

a. Polishing

Medium	Backing Material
colloidal silica	methyl methacrylate
0.1-μm diamond/oil	ground glass
0.5-μm diamond/oil	ground glass
0.3-μm alumina/water	glass
1-μm diamond/oil	bonded to plastic tape

b. Lapping

6-μm diamond/oil	ground glass

was seen. While data taken under all conditions were quite repeatable, the dynamic probe response curves, figure 7, showed that the probe did not attain a stable reading within the measurement window of the data logging equipment. The same general shape for the dynamic probe response was found in similar tests with the remaining probe materials listed in table 2 in this single-probe configuration, and for all probe materials in the two-probe configuration. It was also noted that for all types of probe material, contact resistance values on this specimen were noticeably larger than 10^8 Ω, and it thus became necessary to find a means of lowering these values to the range acceptable for the instrumentation.

For this purpose, a microscope illuminator was used to enhance carrier injection in the area of the contacts for several types of probes. This procedure did reduce the contact resistance by about an order of magnitude, but because it caused a highly erratic dynamic probe response, this illumination procedure was deemed unsatisfactory.

Since the as-received surface on this specimen was not optimal for spreading resistance measurements, further efforts to reduce the contact resistance were concentrated on various specimen surface preparations. Also, since no improvement in terms of reduced contact resistance or better stability was found with any of the alternate probe types, most of the remaining work was done with tungsten-osmium probes. All tests below were done using the two-probe configuration.

b) Effects of Specimen Surface Preparation

The effect of specimen surface preparation on measurement quality was initially tested on the same n-type (silicon-doped, about 7×10^{17} cm^{-3}) GaAs used above. Lapping with 6-μm diamond grit in oil on a frosted glass plate gave a rough or matte surface finish similar to that typically obtained on silicon under the same conditions. Successive improvements in optical quality of the surface were obtained with 0.5- and 0.1-μm diamond, respectively. Figure 8 shows photomicrographs of typical "good" surfaces obtained with each of the above procedures as well as a still more highly polished surface obtained by polishing against 1-μm diamond bonded to plastic film.

It should be noted that it was much more difficult to obtain uniform and reproducible surface quality on GaAs than on silicon with any of the polishing procedures tested. The most significant problem in this regard was the tendency to develop areas of severe, deep scratches or "crumbling" of the GaAs surface. This is illustrated in figure 9.

The measured two-probe resistance values from bulk n-type GaAs specimens after polishing by the methods above did not show a linear correlation with the visual surface quality of the various surfaces. Data taken either on the matte surface (6-μm diamond lap) or on the reasonably well-polished surfaces (0.1-μm diamond on ground glass or 1-μm diamond on plastic tape) were of nearly the same character as on the as-received specimen surface, having average resistances above 10^8 Ω and a dynamic probe response which drifted for the entire period of contact. However, data taken on the specimen polished with 0.5-μm diamond were noticeably improved; i.e., average resistance

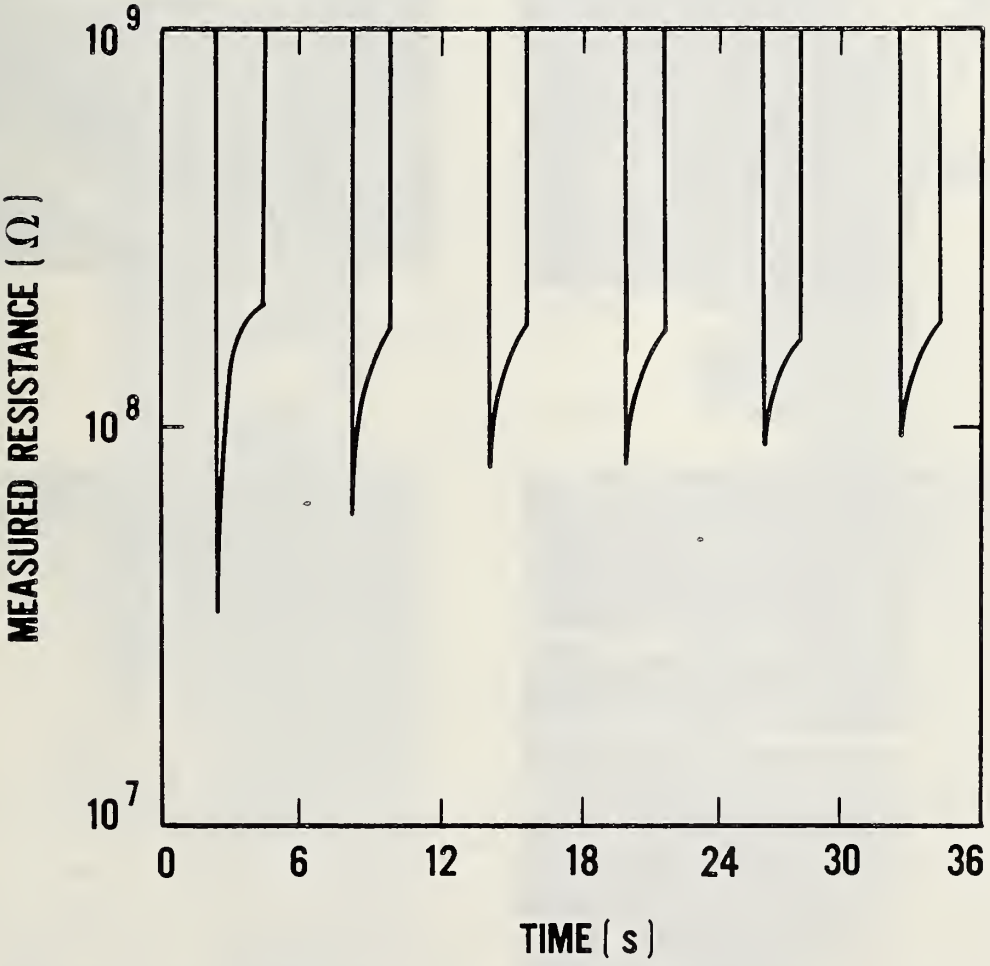

Figure 7. Dynamic probe response for six measurement cycles on silicon-doped bulk GaAs as polished by the manufacturer.

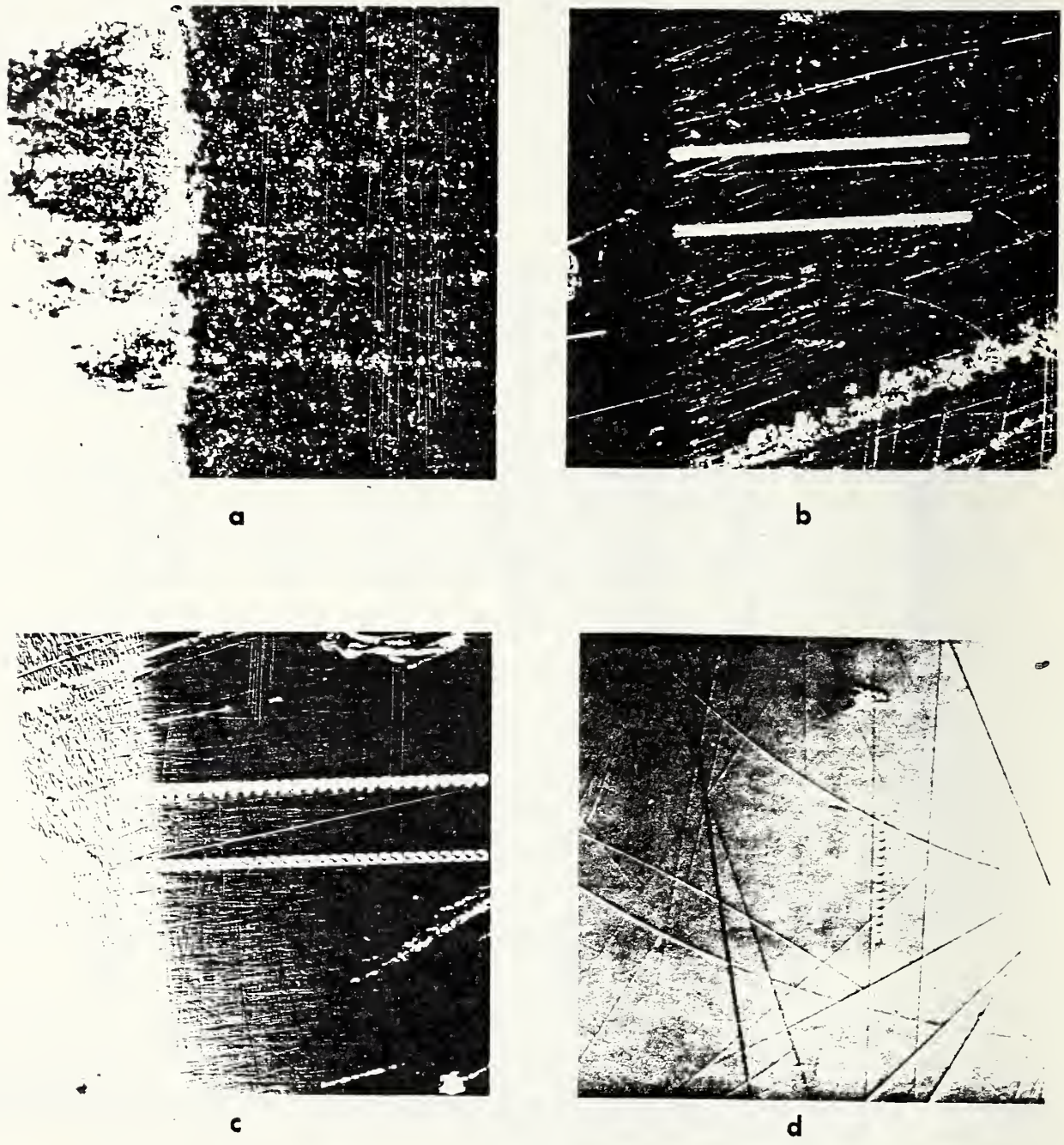

Figure 8. Photomicrographs of typical good surfaces obtained on different bulk GaAs specimens with four preparation procedures: (a) beveled against ground glass with 6-μm diamond, (b) beveled against ground glass with 0.5-μm diamond, (c) beveled against ground glass with 0.1-μm diamond, (d) top surface polished with 1-μm diamond bonded to plastic tape. Parallel tracks in the photomicrographs are damage marks left by the two probes (lateral separation = 60 μm) during measurement.

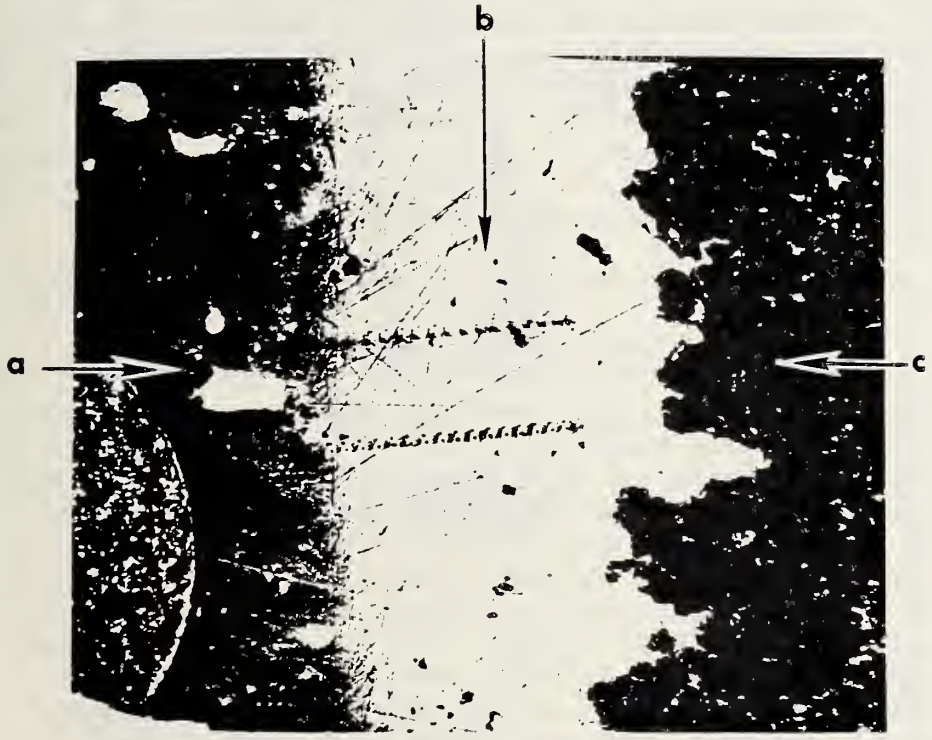

Figure 9. Photomicrograph showing gross surface break-up or crumbling which was sometimes encountered during beveling of GaAs specimens. Three regions can be seen: (a) original top surface showing part of circular ohmic contact (not used), (b) region of reasonable quality surface beveled using 0.5-μm diamond on ground glass, (c) region of severe surface crumbling. Once such crumbling started, it was found to progress in the direction of the bevel edge as more material was beveled away. Lateral separation of probe tracks seen in region (b) is 60 μm.

was decreased by a factor of nearly four, and nearly complete stabilization of the dynamic probe response was obtained within the measurement window.

A direct comparison of two surface finishes and the resulting resistance measurements is given in figure 10. This figure shows surface morphology of a specimen polished at a shallow angle with 0.5-μm diamond on frosted glass subsequent to top-surface polishing with 1-μm diamond bonded to plastic tape, and also some two-probe resistance data from each surface. (The dynamic probe response on the surface polished with 0.5-μm diamond was very similar to that shown for silicon in fig. 6.) This observed dependence of spreading resistance on surface finish does not appear to parallel that found by Queirolo [19] for n-type GaAs. However, it does indicate that at least one diamond-polished surface preparation allows data to be acquired within the 10^8 Ω maximum resistance limit of the instrumentation for n-type GaAs specimens doped in the low- or mid-10^{17} cm^{-3} range. Further, this preparation, polishing with 0.5-μm diamond, is generally compatible with the shallow angle sectioning necessary for profiling implanted layers.

3.6 Experimental Results With Implanted Layers in GaAs

a) Beryllium (p-Type) Layer Profile Data

Initial tests of implanted layer profiling were done on specimens implanted with beryllium. The same lowering of contact resistance after 0.5-μm diamond polishing, previously seen for bulk n-type GaAs, was also seen for these p-type layers. Figure 11 shows the condition of the specimen surface and profile data following beveling with 0.5-μm diamond and with 0.1-μm diamond (both against lapped glass). Figure 12 shows the repeatability of the measurement for four more runs taken on another chip of the same specimen freshly bevel-polished with 0.5-μm diamond. The dynamic probe response data which were taken along with several of these runs showed an unexpected result: the contacts do not really stabilize on the more heavily doped region of the implanted layer, yet they stabilize rather well in the lightly doped deeper-lying region. The mechanism for this effect and its dependence on specimen preparation damage are not known. However, the presence of this effect suggests that the profile data from different regions of the implant may have different reliability. Profile data and dynamic probe response traces were taken on this specimen at probe loads of 20, 30 and 40 grams. No significant dependence of absolute resistance values or character of the dynamic probe response upon probe load was seen. Samples from a second specimen implanted with beryllium under the same implantation conditions and having the same anneal cycle as the first gave two-probe resistance profile data almost identical to that of the first specimen.

b) Calibration of Implanted Layer Profile

An estimate of peak beryllium implant density was obtained by calibrating the probes against three bulk specimens of GaAs doped p-type with zinc. Because of the limited resolution imposed by the measurement repeatability and by the small number of calibration specimens, the dopant density for the bulk calibration specimens was taken from the vendor's Hall effect measurements on adjacent, or nearly adjacent, slices from each of the crystals. These specimens were polished using 0.5-μm diamond on glass so that the surface prepara-

a

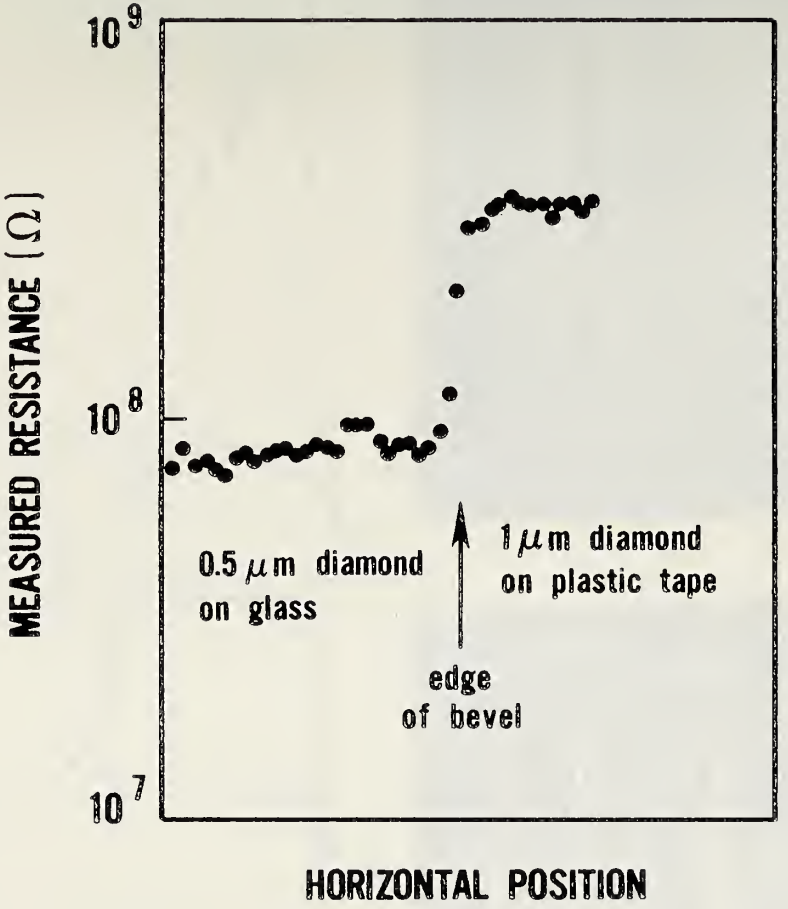

b

Figure 10. Surface finish and spreading resistance data for silicon-doped bulk GaAs specimen which had been top-surface polished with 1-μm diamond bonded by plastic tape and then beveled with 0.5-μm diamond against ground glass; (a) photomicrograph of specimen; the portion polished with 0.5-μm diamond on glass is seen at left of picture; (b) spreading resistance data taken on both surfaces. Probe step increment for tracks seen in figure 10a and for data in figure 10b is 25 μm.

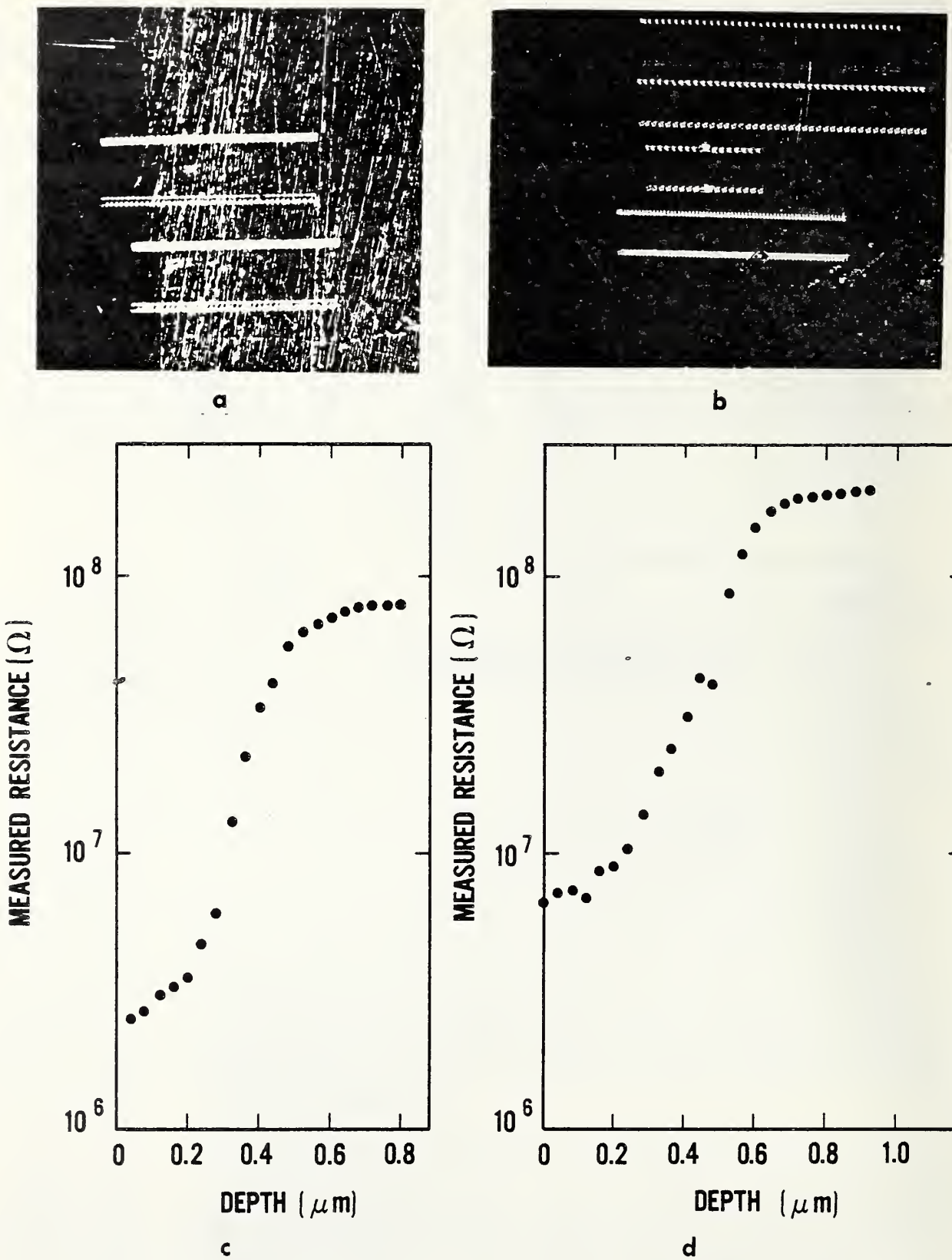

Figure 11. Specimen surface finish and profile data for beryllium-implanted GaAs which has been beveled by two different procedures: (a) and (c) 0.5-μm diamond against lapped glass, (b) and (d) 0.1-μm diamond against lapped glass. Lateral separation of probe tracks in (a) and (b) is 60 μm.

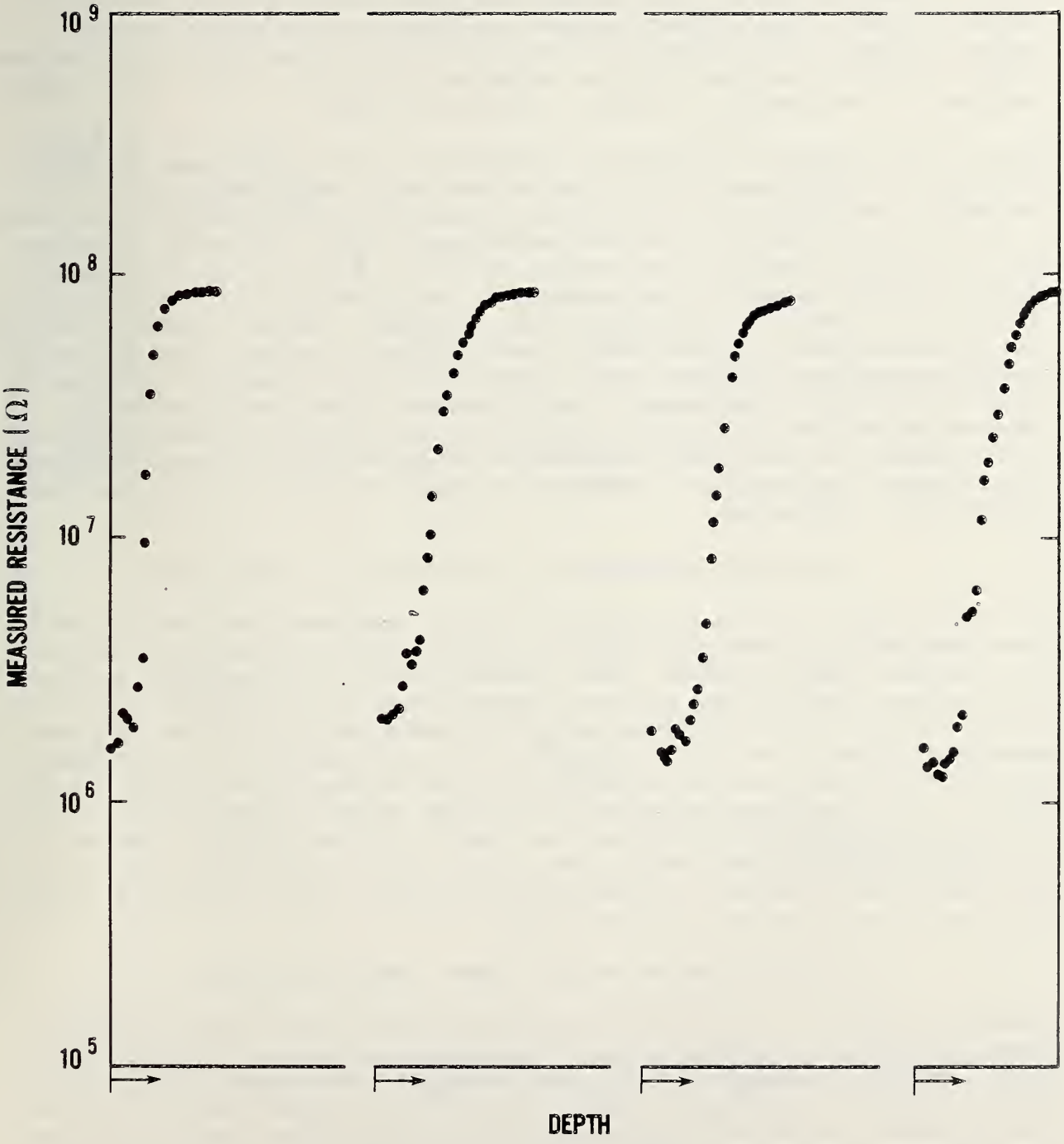

Figure 12. Four sets of spreading resistance depth profile measurement on beryllium-implanted GaAs showing repeatability generally obtained on a specimen beveled with 0.5-μm diamond.

tion would be the same as that on the implanted specimens. The calibration relation was established by piecewise straight-line fitting on a log-log scale of adjacent pairs of two-probe resistance data (from the calibration specimens) to the inverses of the dopant density values for these specimens. The dopant density profile of the ion-implanted layer is then obtained from direct interpolation of its measured resistance values on the calibration scale to obtain dopant density values. No spreading resistance sampling volume correction is applied to the test specimen profile data since, for the reasons stated in section 3.2, the spreading resistance is only a very small component of the measured two-probe resistance values.

Based on the two-probe resistance measurements on these specimens at 30 gf, the peak beryllium density (for profile data taken several weeks prior to arrival of the bulk p-type calibration specimens) was estimated to be between 2×10^{17} and 5×10^{17} cm^{-3} for most measurement sets. This value is noticeably lower than reported by McLevidge [18] for a beryllium layer implanted under identical conditions but annealed at 900°C for 30 min (instead of 800°C for 30 min as used for the present work). However, figure 13 shows a profile indicating noticeably higher dopant density values obtained on one of the beryllium-implanted specimens when it was prepared and measured sequentially with the calibration specimens. The difference in peak beryllium density between the earlier profiles (not shown) and that shown in figure 13 may be due to changes in the probe's calibration response during the several weeks intervening. Nevertheless, reasonable profiles of beryllium-implanted layers appear to be obtainable.

c) Anomalous Differences in Sensitivity to Probe Force

Auxiliary tests on the bulk p-type calibration specimens show that a significant dependence of spreading resistance upon probe force exists for the two more heavily doped specimens, and a moderate probe force dependence exists for the more lightly doped specimen. These probe force dependences were found to exist to about the same extent following beveling of the bulk specimens with either 1- or 0.1-μm diamond or with 3-μm alumina. This result is similar to results obtained on the bulk n-type specimens (sec. 3.5a). However, it is inconsistent with results obtained on the p-type implanted layers on which no probe force dependence was found. It does indicate, however, that the resultant dopant profile of a p-type implanted layer may well depend on probe force, since the calibration scale derived from measurements on bulk GaAs was found to depend on probe force.

d) Silicon and Selenium (n-Type) Layer Profile Data

Efforts to profile silicon- and selenium-implanted layers (n-type) in GaAs were, in general, less successful. This was due in part to the inability to find a surface preparation which would adequately reduce the contact resistance of n-type layers significantly below the 10^8 Ω upper limit of the instrumentation. Based on initial tests on the bulk n-type specimen, even the best surface preparation tested, 0.5-μm diamond polishing, would only allow measurement of dopant density above about 3×10^{17} cm^{-3}. Since two of the three available n-type implanted layers were implanted at relatively low fluences, emphasis was placed on the remaining specimen. This specimen was

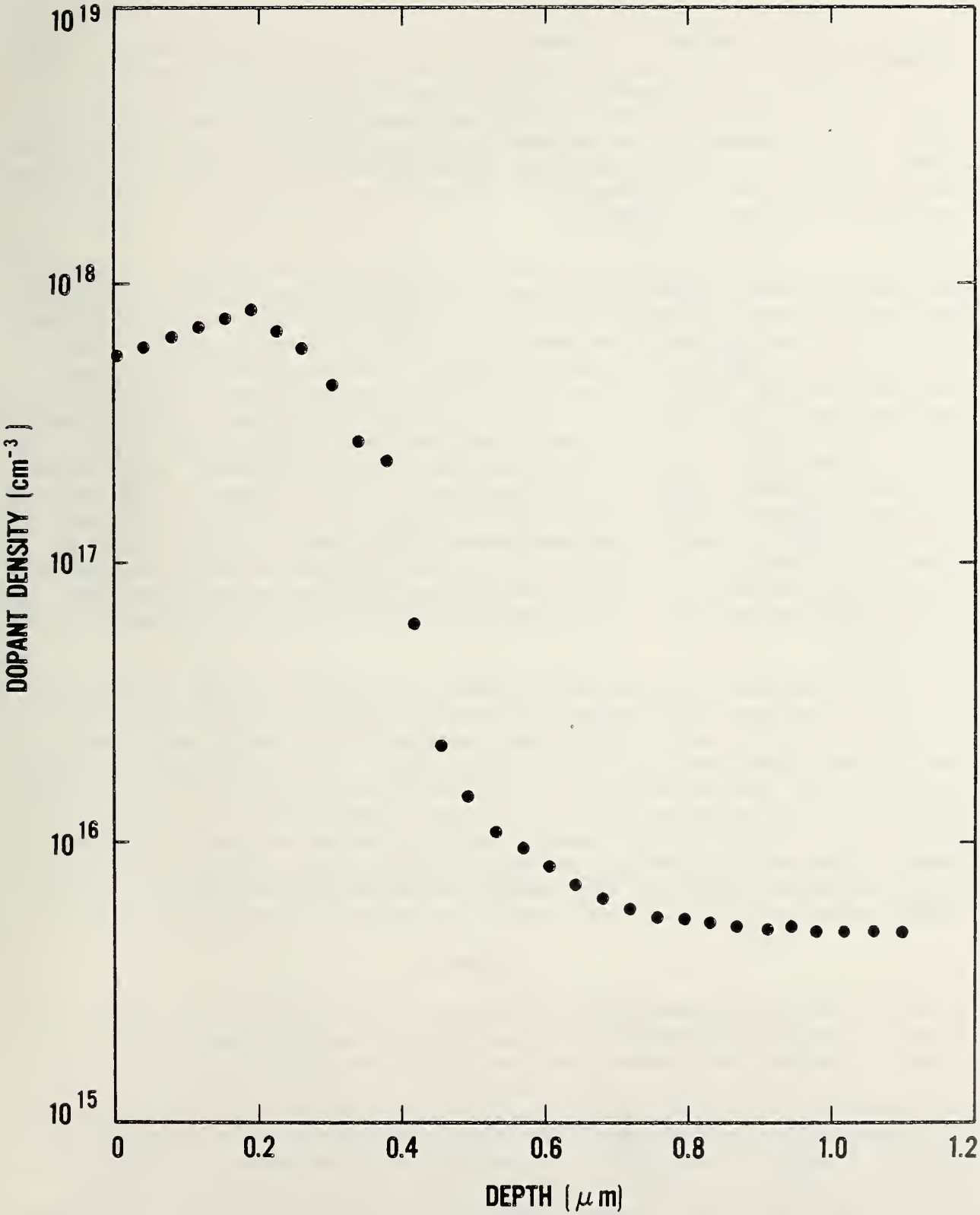

Figure 13. Dopant density depth profile for a beryllium-implanted GaAs specimen beveled with 0.5-μm diamond against ground glass. The apparatus was calibrated using three zinc-doped GaAs bulk specimens beveled in the same manner.

implanted with selenium at a fluence of 5×10^{14} cm^{-2} and was expected from projected range statistics [19] to have a peak dopant density nearly 2×10^{19} cm^{-3}, well in excess of the minimum detectable level estimated above. (Not all of these dopant atoms may have been activated during the anneal cycle, however.) For reference, the predicted dopant profile for this layer, based on the theoretical work of Winterbon [20] is shown in figure 14; the profile of the low-fluence (5×10^{12} cm^{-2}) silicon implant similarly calculated is shown in figure 15.

Based on the resistance profile data from the beryllium-implanted layers, it was expected that the resistance profile of the selenium implant would also be similar in shape to the inverse of the dopant profile (fig. 14). Further, based on the resistance values measured on the bulk n-type specimen (sec. 3.5) and the estimated peak dopant density of the selenium layer, it was expected that the selenium layer would have a minimum value in its resistance profile between 10^5 and 10^6 Ω. Finally, based on the dopant distribution shown in figure 14, all structure in the resistance profile due to the implanted layer should occur within less than 0.3 μm; resistance values should increase to values typical of the substrate, 10^8 Ω or higher, by the end of this depth range. Based on these expectations, no sign of the implanted layer character is seen in the resistance profile data of figure 16a. The shape of the resistance profile data for this specimen changed only marginally despite repeated beveling and remeasurement, including use of various other polishing media and lighter mounting fixtures to reduce damage during beveling.

As further evidence that the small change in resistance values shown in figure 16a is not due to the heavy dose selenium implant, profile data were taken on a silicon layer, figure 16b, implanted at a fluence nearly two orders of magnitude lower than the selenium layer. This specimen was expected to have a peak dopant density (fig. 15) nearly two orders of magnitude less than that of the selenium implant (fig. 14). Nevertheless, its resistance profile has nearly the same shape and absolute values as that of the selenium layer. These data apparently indicate that for n-type implants, the two-probe resistance values are more controlled by mechanisms, possibly lattice damage or surface states, that are not proportional to the dopant density.

3.7 Summary

Spreading resistance measurements on GaAs are very sensitive to surface preparation. This was demonstrated by Queirolo and supported here for different types of preparation; however, the two sets of results are not fully consistent in their particulars. Also, reproducibility of surface quality and of measurement quality, even for a fixed type of preparation, is poorer for GaAs than for silicon. Excess damage and deep scratches, which are atypical of the finish normally produced by a given polishing medium on silicon, occur readily in GaAs and great care must be taken during polishing. Further, Queirolo has stated that changes of the entire calibration curve, by a factor as large as five, have been experienced for a fixed set of probes and a fixed preparation procedure [21].

A nonaqueous specimen surface preparation, polishing with 0.5-μm diamond in oil, was found to give acceptably low resistance values on bulk n- and p-type

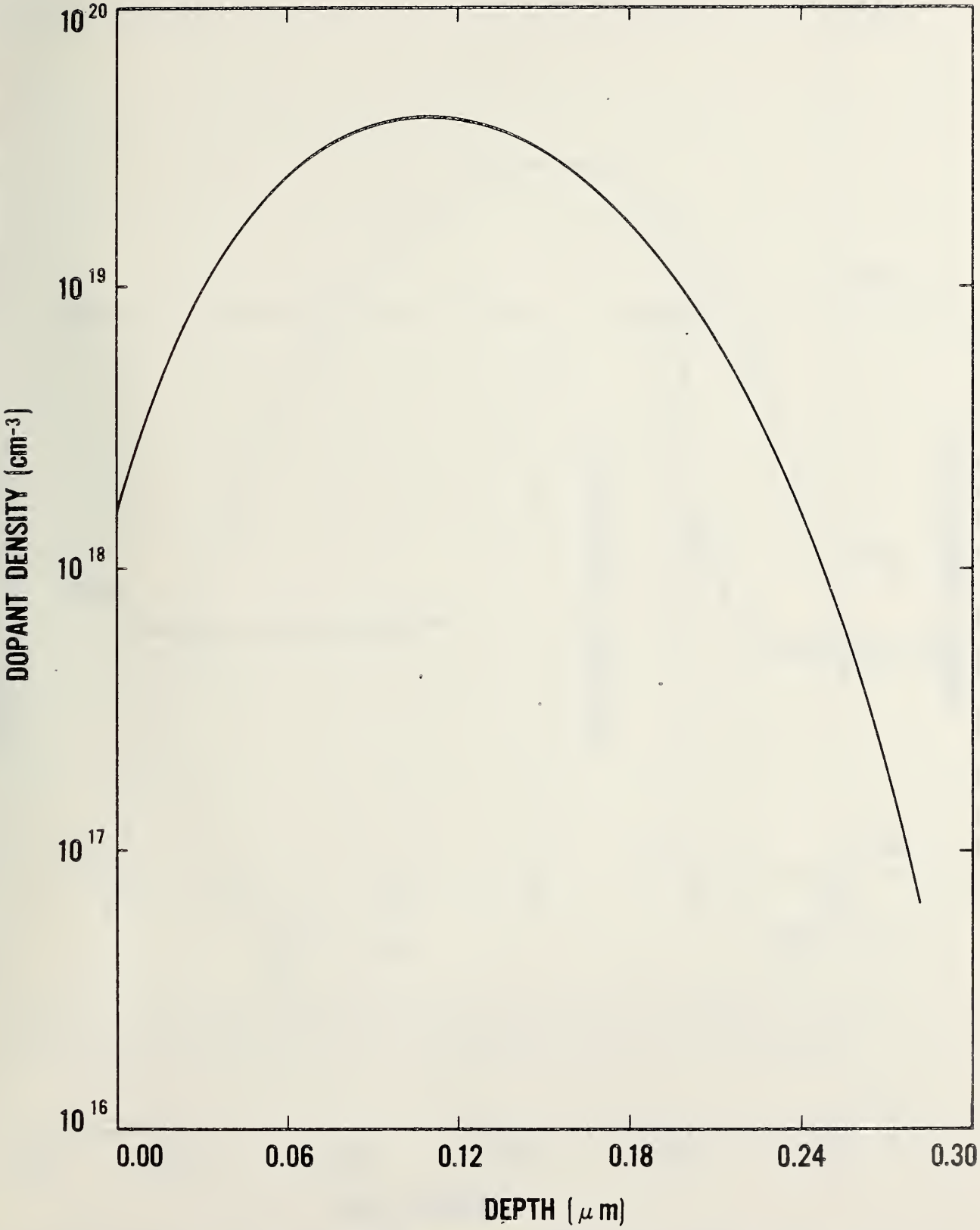

Figure 14. Dopant density profile predicted according to the procedure of Winterbon [20] for the selenium-implanted layer shown in figure 16a. This profile illustrates location of peak density (minimum resistance) and total depth scale expected in data of figure 16a.

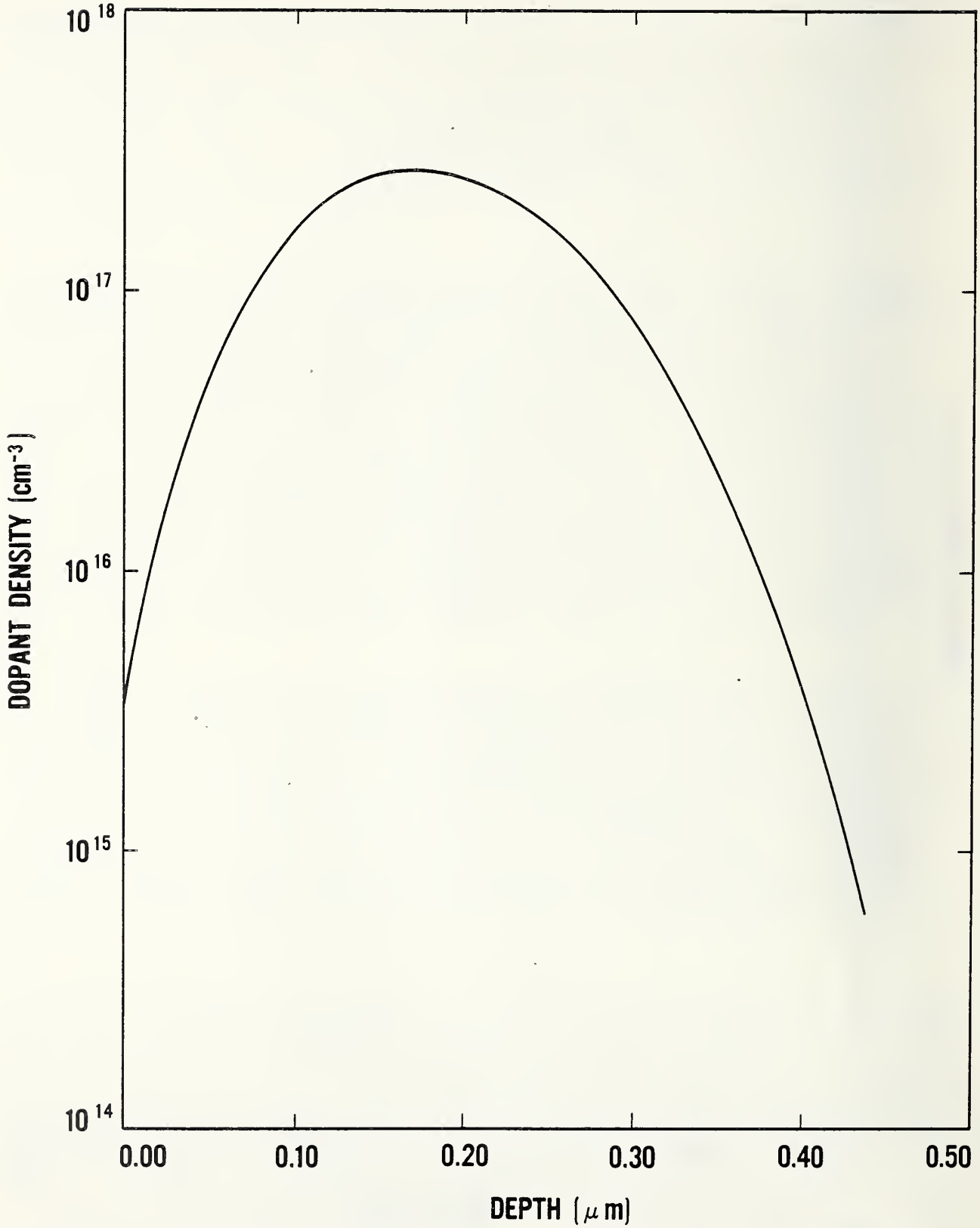

Figure 15. Dopant density profile predicted according to the procedure of Winterbon [20] for the silicon-implanted layer shown in figure 16b. This profile illustrates the location of peak density (minimum resistance) and total depth scale expected in data of figure 16b.

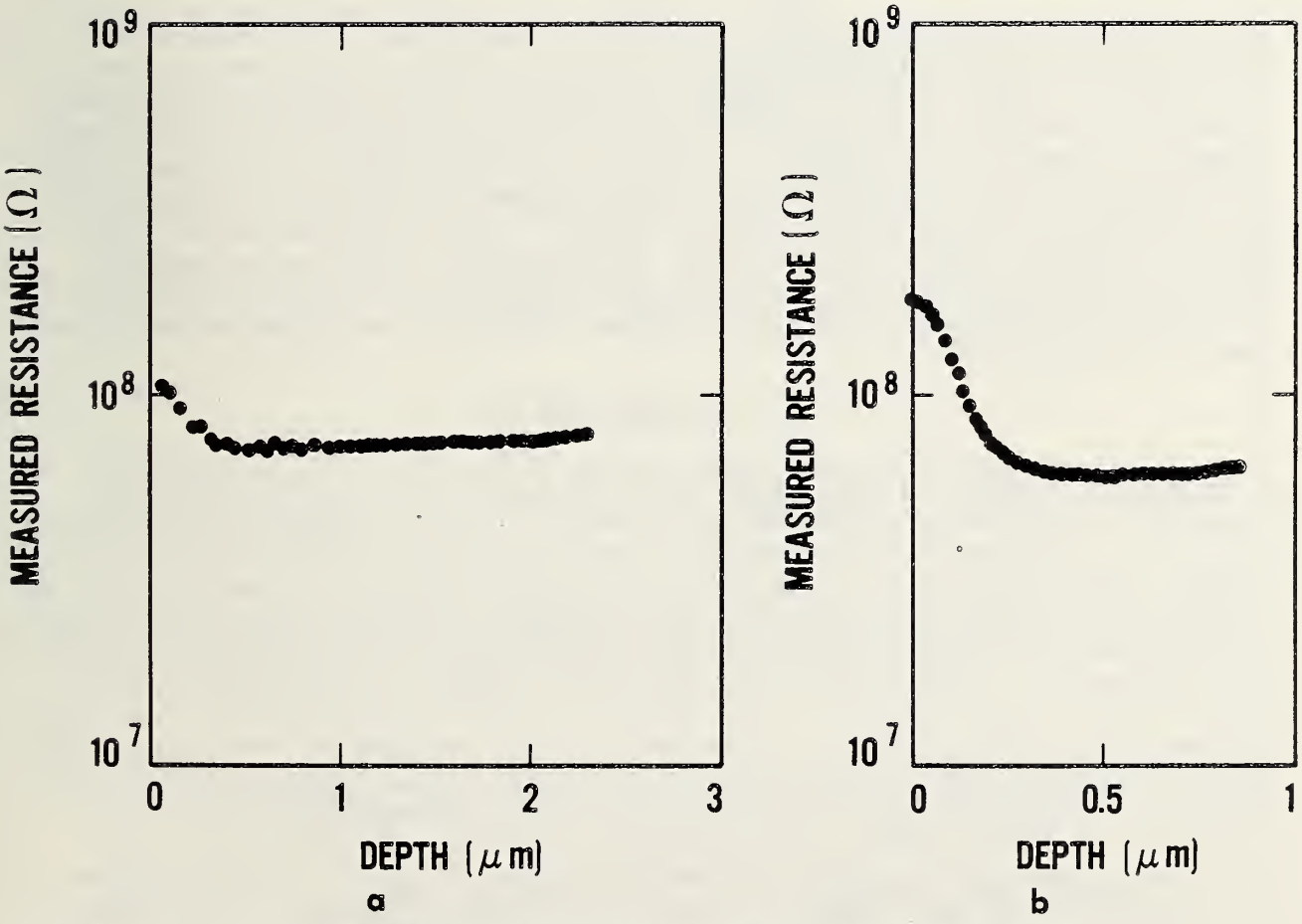

Figure 16. Two-probe resistance profile data for (a) selenium layer implanted into GaAs at 300 keV with a fluence of 5×10^{14} cm^{-2}, and (b) silicon layer implanted into GaAs at 170 keV with a fluence of 5×10^{12} cm^{-2}.

specimens for measurement with commercial spreading resistance equipment. The resistance values obtained with this preparation on the bulk n-type specimen reported in section 3.5 were slightly lower than obtained by Queirolo for a comparably doped specimen prepared with alumina in water. However, values obtained after polishing bulk p-type specimens with 0.5-μm diamond were somewhat higher than those reported by Queirolo for alumina polished p-type bulk specimens. Application of 0.5-μm diamond polishing to implanted specimens showed that measurements on implanted layers of either conductivity type are much less sensitive to probe force than are measurements on comparably polished bulk specimens.

With respect to implanted layers, additional improvement can probably be expected with more extensive testing and refining of surface preparation techniques to reduce residual damage. At present, it is probably desirable to mount calibration chips on the same block as the specimen chip to be sectioned for profiling to attempt to maintain the same surface quality for each piece. The inability to profile n-type implanted layers is not understood. The similarity of measurement results on two n-type implanted layers with widely different dopant densities and the difference between measurement results on these layers and on n-type bulk suggest that the measurement is controlled by the specimen through surface states or damage mechanisms rather than by the probes.

3.8 Recommendation

It appears desirable in any future development of the two-probe spreading resistance technique for application to GaAs to place emphasis on the testing of and the development of an understanding of the parameters which control contact resistance (absolute levels and reproducibility of values) for point pressure contacts. In particular, two questions raised in the present investigation need more detailed study and understanding. The first is the apparent difference in the way specimen preparation damage interacts with thin n-type layers compared with bulk specimens of either conductivity or with thin p-type layers. This question was raised by the inability to obtain satisfactorily low-resistance values on the high fluence n-type implants. The existence of a similar measurement problem should be looked for on n-type diffused and epitaxial layers. These layers are free from concerns over the fraction of dopant activated and from the damage due to fabrication encountered in implanted specimens. The second question relates to the observed difference in probe-force dependence of measured resistance between bulk and thin graded-layer specimens. This difference has great importance for establishing a proper calibration procedure. The possible lack of probe force dependence on all graded layers should likewise be examined on diffused layers to aid in understanding how such an effect may be controlled by dopant profile gradient or intrinsic unannealed damage due to implantation. Once such questions are resolved for relatively thick diffused and epitaxial layers, a more reasonable choice of operating conditions can be made for improving the ability to profile thin implanted layers. Beveling techniques such as the use of chemical or chem-mechanical procedures to minimize induced damage and further alternate probe alloys to reduce contact resistance may also require further investigation.

REFERENCES

1. Aven, M., and Swank, R. K., Ohmic Contacts to Wide Band Gap Semiconductors, *Ohmic Contacts to Semiconductors* (Electrochemical Society, Inc., 1969), pp. 69-81.

2. Van Laar, J., and Scheer, J. J., Influence of Volume Dope on Fermi Level Position at Gallium Arsenide Surfaces, *Surface Science* 8, 342-356 (1967).

3. See, for example, Sze, S. M., *Physics of Semiconductor Devices* (Wiley-Interscience, New York, N.Y., 1969), p. 369.

4. Mead, C. A., and Spitzer, W. G., Fermi Position at Metal-Semiconductor Interfaces, *Phys. Rev.* 134, A713-A716 (1964).

5. Gregory, P. E., Spicer, W. E., Ciraci, S., and Harrison, W. A., Surface State Band on GaAs (100) Face, *Appl. Phys. Lett.* 25, 511-514 (1974).

6. Spicer, W. E., Chye, P. W., Skeath, P. R., Su, C.Y., and Lindau, I., New and Unified Model for Schottky Barrier and III-V Insulator Interface States Formation, *J. Vac. Sci. Technol.* 16, 1422-1432 (1979).

7. Mattauch, R. J., and Green, G., private communication, 1979.

8. Wolfstirn, K. B., and Focht, M. W., Thermoelectric n-p Tester Using ac Bias for Gallium Arsenide and Gallium Phosphide, *Rev. Sci. Instrum.* 42, 152-154 (1971).

9. Neumark, G. F., Fitzpatrick, B. J., Harnack, P. M., Herko, S. P., Kosai, K., and Bhargava, R. N., Potential Profiling as a Means to Determine Conductivity Type: Application to ZnSe, *J. Electrochem. Soc.* 127, 983-985 (1980).

10. Oettinger, F. F., and Larrabee, R. D., Eds., Measurement Techniques for High Power Semiconductor Materials and Devices: Annual Report, October 1, 1978 to September 30, 1979, NBSIR 80-2061 (August 1980).

11. McCombe, B. D., Characterization of III-V Materials, Naval Research Laboratory, NRL Memorandum Report 3701 (February 1978).

12. Frank, H., and Azim, S. A., Measurement of Diffusion Profiles of Zn in *N*-Type GaAs by a Spreading Resistance Technique, *Solid State Electronics* 10, 727-728 (1967).

13. Goodfellow, R. C., Carter, A. C., Davis, R., and Hill, C., New Contact Resistance Profiling Method for the Assessment of III-V Alloy Multilayer Structures, *Electron. Lett.* 14, 328-330 (1978).

14. Queirolo, G., Spreading Resistance Measurements on Gallium Arsenide, *J. Electrochem. Soc.* 125, 1627-1676 (1978).

15. Solid State Measurements, 600 Seco Rd., Monroeville, Pennsylvania.

16. Schumann, P. A., and Gardner, E. E., Spreading Resistance Correction Factors, *Solid State Electronics* 12, 371-375 (1969).

17. Dickey, D. H., and Ehrstein, J. R., *Semiconductor Measurement Technology:* Spreading Resistance Analysis for Silicon Layers with Nonuniform Resistivity, NBS Spec. Publ. 400-48 (May 1978).

18. McLevidge, W. V., Annealing Studies of Beryllium in Gallium Arsenide and Gallium Arsenide Phosphide, Report R-802, Coordinated Science Laboratory University of Illinois, Urbana, Illinois (December 1977).

19. Gibbons, J. F., Johnson, W. F., and Mylroie, S. W., Projected Range Statistics, *Semiconductors and Related Materials,* 2nd ed. (Dowden, Hutchinson and Ross Inc., 1975, distributed by Halstead Press).

20. Winterbon, K. B., Computing Moments of Implanted-Ion Range and Energy Distributions, Report AECL 5536, Chalk River Nuclear Laboratories, Chalk River, Ontario (June 1976).

21. Queirolo, G., private communication.

NBS-114A (REV. 2-8C)

U.S. DEPT. OF COMM. BIBLIOGRAPHIC DATA SHEET (See instructions)	1. PUBLICATION OR REPORT NO. NBSIR 81-2403	2. Performing Organ. Report No.	3. Publication Date December 1981

4. TITLE AND SUBTITLE

Gallium Arsenide Materials Characterization:
Annual Report, October 12, 1978 to October 12, 1979

5. AUTHOR(S)

J. R. Ehrstein and A. C. Seabaugh

6. PERFORMING ORGANIZATION (If joint or other than NBS, see instructions)

NATIONAL BUREAU OF STANDARDS
DEPARTMENT OF COMMERCE
WASHINGTON, D.C. 20234

7. Contract/Grant No.

8. Type of Report & Period Covered
Final, 10/12/78 to 10/12/79

9. SPONSORING ORGANIZATION NAME AND COMPLETE ADDRESS (Street, City, State, ZIP)

Department of the Army
U.S. Army Electronics Technology and Devices Laboratory
Fort Monmouth, NJ 07703

10. SUPPLEMENTARY NOTES

☐ Document describes a computer program; SF-185, FIPS Software Summary, is attached.

11. ABSTRACT (A 200-word or less factual summary of most significant information. If document includes a significant bibliography or literature survey, mention it here)

Ohmic and Schottky barrier contacts for use in electrical characterization were examined both conceptually and experimentally with particular focus on the problems associated with ohmic contacts to semi-insulating GaAs. The conductivity type of the semi-insulating material, which can be either n- or p-type, was investigated by means of a potential profiling technique. In addition, the feasibility of spreading resistance measurements was examined and applied to both low resistivity bulk GaAs and ion-implanted semi-insulating substrate material.

12. KEY WORDS (Six to twelve entries; alphabetical order; capitalize only proper names; and separate key words by semicolons)

Contacts; gallium arsenide; potential profiling; spreading resistance.

13. AVAILABILITY

☒ Unlimited

☐ For Official Distribution. Do Not Release to NTIS

☐ Order From Superintendent of Documents, U.S. Government Printing Office, Washington, D.C. 20402.

☒ Order From National Technical Information Service (NTIS), Springfield, VA. 22161

14. NO. OF PRINTED PAGES
38

15. Price
$6.50